Original Article

MOLECULAR METABOLISM

Hepatic ketogenesis is not required for starvation adaptation in mice

Kyle Feola[1], Andrea H. Venable[2], Tatyana Broomfield[2], Morgan Villegas[3], Xiaorong Fu[3], Shawn Burgess[1,3], Sarah C. Huen[1,2,*]

ABSTRACT

Objective: In response to bacterial inflammation, anorexia of acute illness is protective and is associated with the induction of fasting metabolic programs such as ketogenesis. Forced feeding during the anorectic period induced by bacterial inflammation is associated with suppressed ketogenesis and increased mortality. As ketogenesis is considered essential in fasting adaptation, we sought to determine the role of ketogenesis in illness-induced anorexia.

Methods: A mouse model of inducible hepatic specific deletion of the rate limiting enzyme for ketogenesis (HMG-CoA synthase 2, *Hmgcs2*) was used to investigate the role of ketogenesis in endotoxemia, a model of bacterial inflammation, and in prolonged starvation.

Results: Mice deficient of hepatic *Hmgcs2* failed to develop ketosis during endotoxemia and during prolonged fasting. Surprisingly, hepatic HMGCS2 deficiency and the lack of ketosis did not affect survival, glycemia, or body temperature in response to endotoxemia. Mice with hepatic ketogenic deficiency also did not exhibit any defects in starvation adaptation and were able to maintain blood glucose, body temperature, and lean mass compared to littermate wild-type controls. Mice with hepatic HMGCS2 deficiency exhibited higher levels of plasma acetate levels in response to fasting.

Conclusions: Circulating hepatic-derived ketones do not provide protection against endotoxemia, suggesting that alternative mechanisms drive the increased mortality from forced feeding during illness-induced anorexia. Hepatic ketones are also dispensable for surviving prolonged starvation in the absence of inflammation. Our study challenges the notion that hepatic ketogenesis is required to maintain blood glucose and preserve lean mass during starvation, raising the possibility of extrahepatic ketogenesis and use of alternative fuels as potential means of metabolic compensation.

Keywords Ketogenesis; Starvation adaptation; Fasting metabolism; HMGCS2; Endotoxemia

1. INTRODUCTION

Physio-behavioral responses to infection and inflammation such as anorexia are part of a collection of sickness behaviors that are evolutionarily conserved across many species [1]. We previously showed that feeding mice during the period of anorexia has divergent effects on survival in bacterial, viral, and parasitic infections [2,3]. In bacterial infection or sterile inflammation modeled by lipopolysaccharide (LPS) endotoxemia, we found that feeding, specifically glucose supplementation, promotes mortality [2], suggesting an inherent protective effect of anorexia and fasting metabolism.

Hepatic ketogenesis is an obvious candidate for the protective effects of starvation because its induction during fasting results in millimolar concentrations of acetoacetate and β-hydroxybutyrate in circulation. These ketones are derived from the catabolism of fatty acids, but unlike fatty acids, they are universal substrates for nearly all oxidative cells. As a fundamental fasting adaptation metabolic pathway, ketogenesis is considered vital to surviving prolonged starvation. The key role of ketogenesis during nutrient scarcity is to supply energy to glucose-dependent tissues such as the brain, while sparing gluconeogenesis, which in turn minimizes protein catabolism for gluconeogenic substrate. As the reduction in protein catabolism during prolonged starvation is mandatory for survival, ketogenesis is thus considered indispensable in mammalian metabolic starvation adaptation. In addition to being an alternative fuel, ketones also act as signaling molecules, mediate post translational protein modification, and attenuate inflammatory and oxidative stress responses [4]. Since ketogenesis is rapidly suppressed by glucose supplementation, we hypothesized that ketones mediate the protective effect of anorexia induced during bacterial inflammation.

Mitochondrial 3-Hydroxy-3-Methylglutaryl-CoA Synthase 2 (HMGCS2) is the rate-limiting enzyme required for ketogenesis. We previously showed that liver HMGCS2 is required for the generation of circulating ketones during fasting [5]. Specifically, mice with inducible hepatocyte-specific deletion of *Hmgcs2* were unable to develop fasting ketosis. Using this mouse model of hepatic ketogenic deficiency, we sought to examine the role of ketogenesis in organismal survival in response to bacterial inflammation. Despite a period of anorexia

[1]Department of Pharmacology, University of Texas Southwestern Medical Center, Dallas, TX 75390, USA [2]Department of Internal Medicine (Nephrology), University of Texas Southwestern Medical Center, Dallas, TX 75390, USA [3]Center for Human Nutrition, University of Texas Southwestern Medical Center, Dallas, TX 75390, USA

*Corresponding author. 5323 Harry Hines Blvd., Dallas, TX 75390-9041, USA. E-mail: sarah.huen@utsouthwestern.edu (S.C. Huen).

Received April 17, 2024 • Revision received June 4, 2024 • Accepted June 10, 2024 • Available online 12 June 2024

https://doi.org/10.1016/j.molmet.2024.101967

induced by LPS, mice with hepatic ketogenic deficiency and an inability to induce ketosis demonstrate no difference in survival from endotoxemia compared to their wild-type littermates. We subsequently observed that hepatic ketogenesis is surprisingly not required for prolonged starvation adaptations.

2. MATERIAL AND METHODS

2.1. Mice

All animal experiments were performed in accordance with institutional regulations after protocol review and approval by Institutional Animal Care and Use Committees at University of Texas Southwestern Medical Center. *Alb-CreERT2;Hmgcs2$^{fl/fl}$* (or Alb^{Hmgcs2KO}) and *Six2-Cre;Hmgcs2$^{fl/fl}$* mice were generated as previously described [5]. Alb^{Hmgcs2KO} mice (10–12 weeks old) and *Hmgcs2$^{fl/fl}$* littermate controls were gavaged once with tamoxifen in peanut oil (70 mg/kg body weight, Sigma). The MITO-Tag mice [6] were bred with *Pvalb-Cre* [7] mice to generate a mouse model *PvAlb-Cre;MITO-Tag* (or PvAlb-MT) with distal convoluted tubule specific [8] mitochondrial tags. The MITO-Tag construct contains GFP which was used for cell-specific mitochondrial immunostaining. C57BL/6J (RRID:IMSR_JAX:000664), MITO-Tag (RRID:IMSR_JAX:032290) and *Pvalb-Cre* (RRID:IMSR_JAX:017320) mice were purchased from Jackson Laboratory. All mouse strains were maintained on a C57BL/6 background and housed under standard laboratory conditions with a 12 h light:dark cycle.

2.2. Murine endotoxemia model

Mice were injected intraperitoneally with 10 mg/kg of LPS derived from *Escherichia coli* 055:B5 (Sigma–Aldrich, L2880) diluted in (10*body weight) μL of sterile PBS. During endotoxemia, if a mouse was unable to right itself or had a temperature below 23 °C, the mouse was humanely euthanized.

2.3. Mouse fasting experiments

Mice were provided *ad libitum* access to water and standard chow (Harlan Teklad, 2916) or fasted for up to 72 h or 96 h and then re-fed. During the fasting period, if a mouse lost more the 30% of baseline body weight or had a temperature below 23 °C, the mouse was humanely euthanized.

2.4. Plasma metabolite measurements

Blood glucose and blood ketones (beta-hydroxybuytrate, BOHB) were determined by whole blood via tail vein prick and measured via glucometer (OneTouch) and ketone meter (Keto-Mojo), respectively. For other tests, retro-orbital or submandibular blood was harvested, and plasma was isolated using lithium heparin coated plasma separator tubes (BD). Plasma non-esterified fatty acid concentration was measured using a kit according to the manufacturer's protocols (Wako Diagnostics). Plasma total ketones and BOHB were measured using enzymatic colorimetric assay kits (Wako Diagnostics), and acetoacetate (AcAc) levels were calculated based on the difference between total ketones and BOHB.

For plasma amino acids analysis, thawed plasma samples were immediately spiked with labeled amino acid internal standards (Cambridge Isotope Laboratories, Inc., Sigma–Aldrich) and cold acetone. The extraction and derivatization of amino acids from liver were prepared as previously described [9]. The separation of amino acids was achieved on a reverse phase C18 column (Xbridge, Waters, Milford, MA; 150 × 2.1 mm, 3.5 μm) with a gradient elution. Amino acids were detected using the MRM mode by monitoring specific transitions under positive electro spray on Triple Quad™ 5500+ QTrap LC/MS/MS mass spectrometer (Applied Biosystems/Sciex Instruments). Quantification was done by comparison of individual ion peak areas to that of an internal standard.

To measure organic acids in plasma, 50 μl plasma was mixed with labeled organic acid internal standards (Cambridge Isotope Laboratories, Inc., Isotec, Sigma–Aldrich), 350 μl of 0.8% sulfosalicylic acid and 50 μl of 5 M hydroxylamine-HCl solution, and then centrifuged (21,000 g, 10 min, 4 °C). The supernatant was neutralized with 2 M KOH to pH 6–7 and then incubated at 65 °C for 60 min. The reaction mixture was acidified using 2 M HCl (pH 1–2), saturated with sodium chloride, and extracted with ethyl acetate. The dried extract was dissolved with acetonitrile and MTBSTFA as silylation reagent and incubated at 60 °C for 60 min. The derivatives were analyzed by Agilent 7890A gas chromatograph interfaced to an Agilent 5975C mass-selective detector (70 eV, electron ionization source). An HP-5ms GC column (30 m × 0.25 mm I.D., 0.25 μm film thickness) was used for all analysis [10].

Plasma acetate was measured by gas chromatography/mass spectrometry (GC/MS) via the UT Southwestern Children's Medical Center Research Institute Metabolomics Facility. The measurement protocol was modified based on methods described by Tumanov et al. [11]. Briefly, 40 μl of plasma samples were run on a GC/MS (Agilent Technologies, #5977A) with Zebron ZB-1701 GC Columns (Phenomenex, #7HG-G006-11). A standard curve was prepared and run with the samples. The curve was a 12-point standard curve for quantitation with 20 μl of 1 mM d_3-sodium acetate (Sigma, 176079), 0–70 μl of 1 mM sodium acetate (Sigma–Aldrich; S2889) and Optima LC/MS grade water to bring the final volume to 100 μl. Using the quantitation standard curve as a guide for retention times, the peaks that were monitored across all samples were m/z 61 and 64 representing ^{12}C-acetate and d_3-acetate, respectively. Concentrations were calculated using the standard curve.

2.5. Metabolic chamber studies

Energy expenditure and oxygen consumption before and after fasting were measured by indirect calorimetry using metabolic chambers (TSE via the UT Southwestern Metabolic Phenotyping Core). A 4-day period of acclimation was followed by 2 days of ad libitum feeding recording prior to fasting. After 2 days of baseline recordings, food was removed and recordings were continued for 72 h.

2.6. Body composition analyses

Lean and fat mass were measured by nuclear magnetic resonance (NMR) use an EchoMRI-100 analyzer. For liver glycogen measurements, livers were rapidly harvested from ad libitum fed WT and Alb^{Hmgcs2KO} mice 72 h after oral tamoxifen administration, immediately flash frozen in liquid nitrogen, and then stored in −80 °C. Liver glycogen was then measured using a colorimetric assay (Abcam ab65620) following manufacturer's instructions. Liver triglycerides were extracted using the Folch Method [12] and assayed using Triglycerides Reagent (Thermo Scientific TR22421) in conjunction with the Matrix Plus Chemistry Reference Kit (Verichem Laboratories 9500). Briefly, liver was weighed before flash freezing, followed by suspension in 1 mL Folch solution (2:1 chloroform:methanol) and bead homogenized in Fisherbrand™ Pre-Filled Bead Mill Tubes using a Fisherbrand™ Bead Mill 24 Homogenizer. Homogenates were transferred to glass tubes, and bead tubes were washed with an additional 1 mL of Folch solution followed by combination with homogenates. An additional 3 mL of Folch solution and 1 mL of PBS were added to glass tube followed by vortexing. Tubes were then centrifuged at 1500 × *g* for 10 min, and the lower phase containing triglycerides was collected and

transferred to a new vial. 80 μl of this solution was aliquoted and dried by nitrogen jets. Dried samples and standards were then resuspended in triglycerides reagent and measured per the manufacturer's protocol. Final tissue concentrations were normalized to extracted tissue weight.

2.7. RNA extraction and quantification

For tissue RNA extraction, tissues were harvested into RNA-STAT RNA isolation reagent (Tel Test, Inc) and disrupted by bead homogenization. RNA was extracted using Direct-Zol (Zymo Research) kits per manufacturer's protocol. cDNA synthesis was performed using MMLV reverse transcriptase (Clontech) with oligo(dT) primers. qRT-PCR reactions were performed on a QuantStudio7 Flex (Applied Biosystems) using iTaq™ Universal SYBR Green Supermix (Bio-Rad). Transcript levels were normalized to *Rpl13a*. Primers (Sigma) used for qRT-PCR are listed in Supplemental Table 1.

2.8. Immunoblot

Harvested tissues were snap-frozen in liquid nitrogen then bead homogenized in either RIPA buffer (Teknova) for liver, heart and kidney tissues or N-PER™ Neuronal Protein Extraction Reagent for brain samples (ThermoFisher), both supplemented with HALT protease and phosphatase inhibitors (ThermoFisher). 30 μg of protein/sample were loaded into 4–20% Mini-PROTEAN TGX stain-free polyacrylamide gels (Bio-Rad), transferred onto activated PVDF membrane (Bio-Rad), blocked in 5% milk in TBST for 30 min, and incubated with primary antibodies (Supplemental Table 2) overnight at 4 °C. Membranes were washed, then incubated with secondary antibodies for 1 h at room temperature. Protein was visualized using enhanced chemiluminescence reagent (Bio-Rad) and densitometry determined based on total protein in Image Lab (Bio-Rad).

2.9. Immunostaining

Kidneys were harvested and fresh frozen in OCT for immunofluorescent staining. Kidney sections (6 μm) were fixed with 4% PFA for 30 min and blocked in 5% normal donkey serum for 1 h at room temperature. For brain immunostaining, mice underwent cardiac perfusion fixation with 10% neutral buffered formalin. The brain was harvested and fixed with 10% neutral buffered formalin overnight at 4 °C and then incubated in 30% sucrose in PBS until the tissue submerged. Brain sections were embedded in OCT and 6 μm cryosections were blocked with 5% normal donkey serum and 3% Triton X-100 for 1 h at room temperature. Primary antibodies (Supplemental Table 2) were incubated overnight at 4 °C and secondary antibodies were incubated for 1 h at room temperature. Images were taken with a Nikon Eclipse 80i microscope using a Nikon DS-Fi3 camera or Keyence BZX-800 microscope and processed in ImageJ.

2.10. Statistics

Statistical analyses were performed using Prism 10.0 (GraphPad). Mantel–Cox log rank test was used to compare survival curves. Student's unpaired two-way t-test and two-way ANOVA with Sidak's multiple comparison analysis were used when appropriate. Data expressed as mean ± SD. A P value ≤ 0.05 was considered statistically significant.

3. RESULTS AND DISCUSSION

3.1. Circulating liver-derived ketones are not required for surviving endotoxemia

Although ketogenesis during endotoxemia is blunted when compared directly to fasting ketosis in the absence of inflammation or infection [13–15], mice developed a period of anorexia that is associated with ketosis in response to LPS (Figure 1A, B). We previously showed that glucose supplementation suppressed LPS-induced ketosis and increased mortality [2]. We proposed that ketogenesis was mediating the protective effects of sickness-induced anorexia in bacterial inflammation. However, whether ketosis secondary to LPS-induced anorexia is a protective response is unsettled. To assess the role of circulating ketones in sepsis, we used a mouse model with inducible hepatic-specific *Hmgcs2* deletion (*Alb-CreERT2;Hmgcs2$^{fl/fl}$*, or Alb^{Hmgcs2KO}) as previously described [5]. Two weeks after tamoxifen administration in adult mice, hepatic HMGCS2 protein abundance was decreased by 99.97 ± 0.006% in both ad libitum fed and 24-h fasted Alb^{Hmgcs2KO} (Figure 1C). The Alb^{Hmgcs2KO} does not affect HMGCS2 in extrahepatic organs (Figure 1D and [5]). While HMGCS2 deficiency in humans, germline *Hmgcs2* deletion in mice, or short term *Hmgcs2* knockdown in neonatal mice results in hepatomegaly and hepatic steatosis [16–18], ad libitum fed liver wet weights and hepatic triglyceride (TG) content did not differ between Alb^{Hmgcs2KO} mice and wild-type littermates (Figure 1E, Supplemental Figure 1A). The lack of hepatic steatosis two weeks after tamoxifen induced hepatic *Hmgcs2* deletion is consistent with a model of short-term *Hmgcs2* knockdown in adult mice on standard chow [18].

We confirmed that, similar to fasting [5], Alb^{Hmgcs2KO} mice were incapable of increasing plasma total ketone levels in response to LPS (Figure 1F). Given the association between glucose-induced suppression of ketogenesis and increased mortality during endotoxemia, we next asked whether Alb^{Hmgcs2KO} mice would be more susceptible to LPS mortality due to the lack of ketone production. Interestingly, despite the inability to induce ketosis in response to a LPS challenge, both male and female Alb^{Hmgcs2KO} mice did not fare worse than their littermate controls (Figure 1G). Alb^{Hmgcs2KO} mice also maintained their body temperatures, similar to wild-type controls (Figure 1H). While ketosis is thought to preserve fasting glycemia by providing abundant alternative fuel [4], it is surprising that Alb^{Hmgcs2KO} mice were able to maintain similar blood glucose levels compared to wild-type mice and were able to recover from LPS-induced hypoglycemia (Figure 1I). Thus, although suppression of ketogenesis by forced feeding in the context of inflammation-induced anorexia is associated with increased mortality, ketosis is not required for surviving bacterial inflammation.

3.2. Hepatic ketogenesis is not required for starvation adaptation

Ketogenesis is considered indispensable in mammalian metabolic starvation adaptation. LPS induced anorexia can last 24–72 h (Figure 1A), and yet Alb^{Hmgcs2KO} mice are able to adapt without significant morbidity or mortality. Previous studies using a model of systemic *Hmgcs2* anti-sense oligonucleotide (ASO) knockdown proposed that ketone metabolism plays a more important role in preserving hepatic intermediary metabolism than providing energy to extrahepatic organs [18]. However, these studies examined overnight fasting periods or metabolic conditions in the context of overnutrition using a high fat diet model. Thus, we next examined whether Alb^{Hmgcs2KO} mice could tolerate prolonged starvation without an inflammatory stimulus. Similar to a LPS challenge, both male and female Alb^{Hmgcs2KO} mice developed similar levels of hypoglycemia compared to littermate controls during 72 h of fasting, despite the lack of ketosis (Figure 2A, B). Alb^{Hmgcs2KO} mice and controls lost the same amount of body weight during fasting (Figure 2C). Body temperatures trended lower in female Alb^{Hmgcs2KO} mice during the 72-h fasting period, however, at each individual time point, the body temperatures did not reach statistical significance (Figure 2D). As expected, the fasting-inductions of β-hydroxybutyrate (BOHB) and acetoacetate (AcAc) blood concentrations were lost in

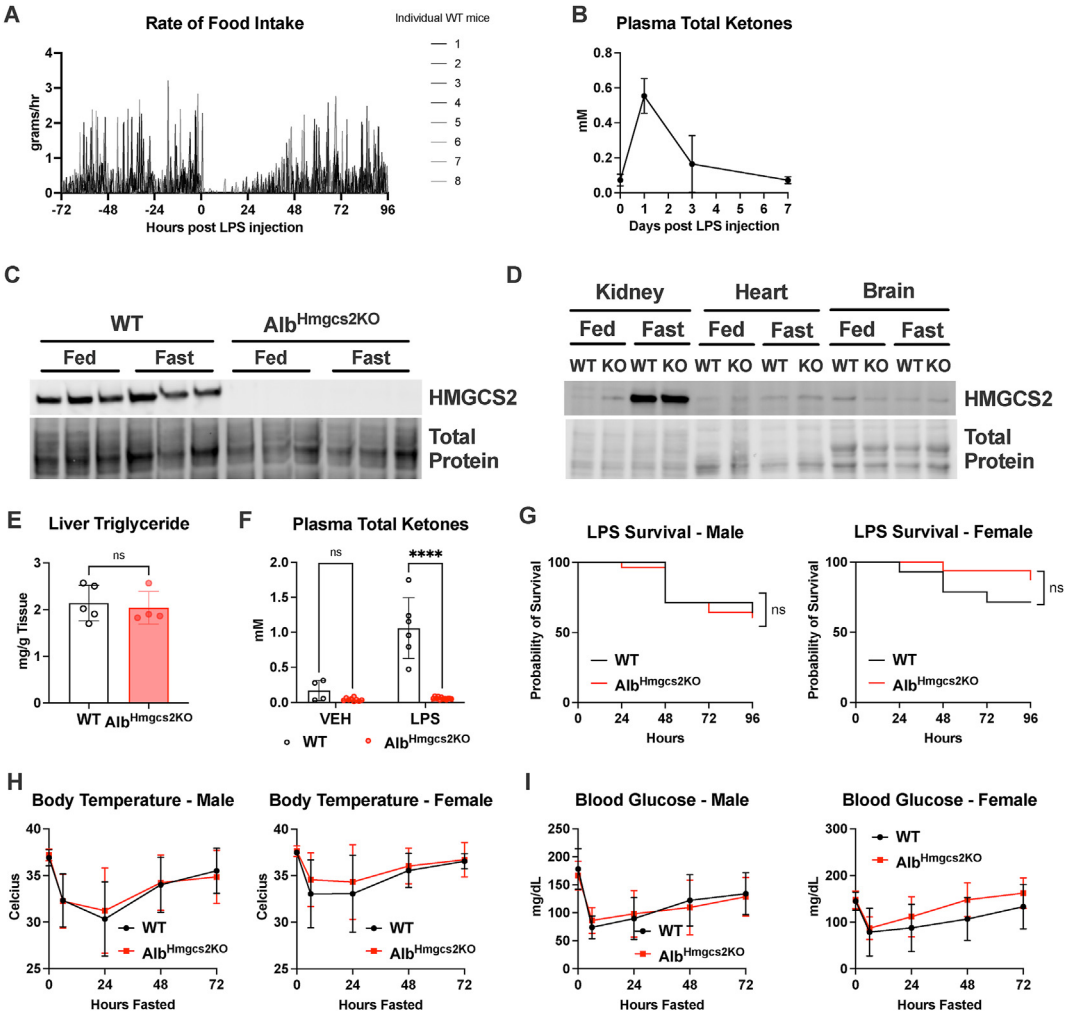

Figure 1: Lack of ketosis does not affect survival from endotoxemia. **(A–B)** C57BL/6J mice were challenged with 10 mg/kg i.p. LPS. **(A)** Food intake shown as grams per hour. n = 8. **(B)** Plasma total ketones after LPS challenge. n = 7. **(C–D)** WT and Alb^{Hmgcs2KO} (KO) mice were ad libitum fed or fasted for 24 h 2 weeks after tamoxifen administration. Whole tissue protein lysates immunoblotted for HMGCS2. **(E)** Liver triglyceride concentrations (mg/g tissue) in ad libitum fed mice 2 weeks after tamoxifen administration. n = 4–5/group. **(F)** Plasma total ketones 24 h after PBS vehicle or 10 mg/kg i.p LPS challenge. n = 4–11/group. **(G–I)** WT and Alb^{Hmgcs2KO} mice were challenged with 10 mg/kg i.p. n = 28/group (male), n = 14–16/group (female). **(G)** Kaplan–Meier survival curve. **(H)** Rectal body temperatures. **(I)** Blood glucose. Data expressed as mean ± SD, $^{****}P < 0.0001$, ns (not significant); two sided unpaired t-test (E), two-way ANOVA with Sidak's multiple comparisons test (F) with mixed effects (H, I), Mantel–Cox test (G).

Alb^{Hmgcs2KO} mice, but the loss of ketogenesis had no effect on circulating non-esterified fatty acids during fasting (Figure 2E). As we did not observe any mortality with 72 h of fasting, we next assessed the survival of Alb^{Hmgcs2KO} mice during a prolonged 96-h fast with refeeding. Surprisingly, female Alb^{Hmgcs2KO} mice exhibited no difference in survival compared to wild-type littermates, while the male Alb^{Hmgcs2KO} mice had better survival (Figure 2F).

3.3. Hepatic ketogenesis does not preserve lean mass during prolonged fasting

Starvation ketosis has long been thought to provide a non-carbohydrate fuel for the brain's energy needs, thus decreasing glucose consumption and sparing the mobilization of muscle protein as a source of gluconeogenic substrate [19]. To assess the changes in lean muscle mass in Alb^{Hmgcs2KO} mice, we measured whole body composition before and during a 72-h fast. Interestingly, both male and female Alb^{Hmgcs2KO} mice exhibited similar lean muscle mass loss compared to WT littermates throughout the fasting period (Figure 3A–C). There were no significant differences in the expression of proteolysis genes known to be differentially regulated during fasting [20] between Alb^{Hmgcs2KO} mice and WT mice (Figure 3D). Although we did not observe a difference in liver and adipose tissue wet weights at baseline and after 24 h of fasting between Alb^{Hmgcs2KO} and WT male mice (Supplemental Figure 1A), we observed that male, but not female Alb^{Hmgcs2KO} mice had higher absolute fat mass at baseline, prior to the fast, as measured by whole body NMR (Figure 3E, F). However, both male and female Alb^{Hmgcs2KO} mice lost a lower percent of fat mass over the 72-h fast (Figure 3G). To better understand the apparent discordance between the difference in fat mass loss compared to the lack of differences in body weight and lean mass, the absolute body weight, fat mass and lean mass differences were compared (Supplemental Tables 3 and 4). The body weight and lean mass differences between the Alb^{Hmgcs2KO} and WT mice are small relative to the overall body weight and lean mass, while the fat mass difference is large in proportion to the overall fat mass. While there was a

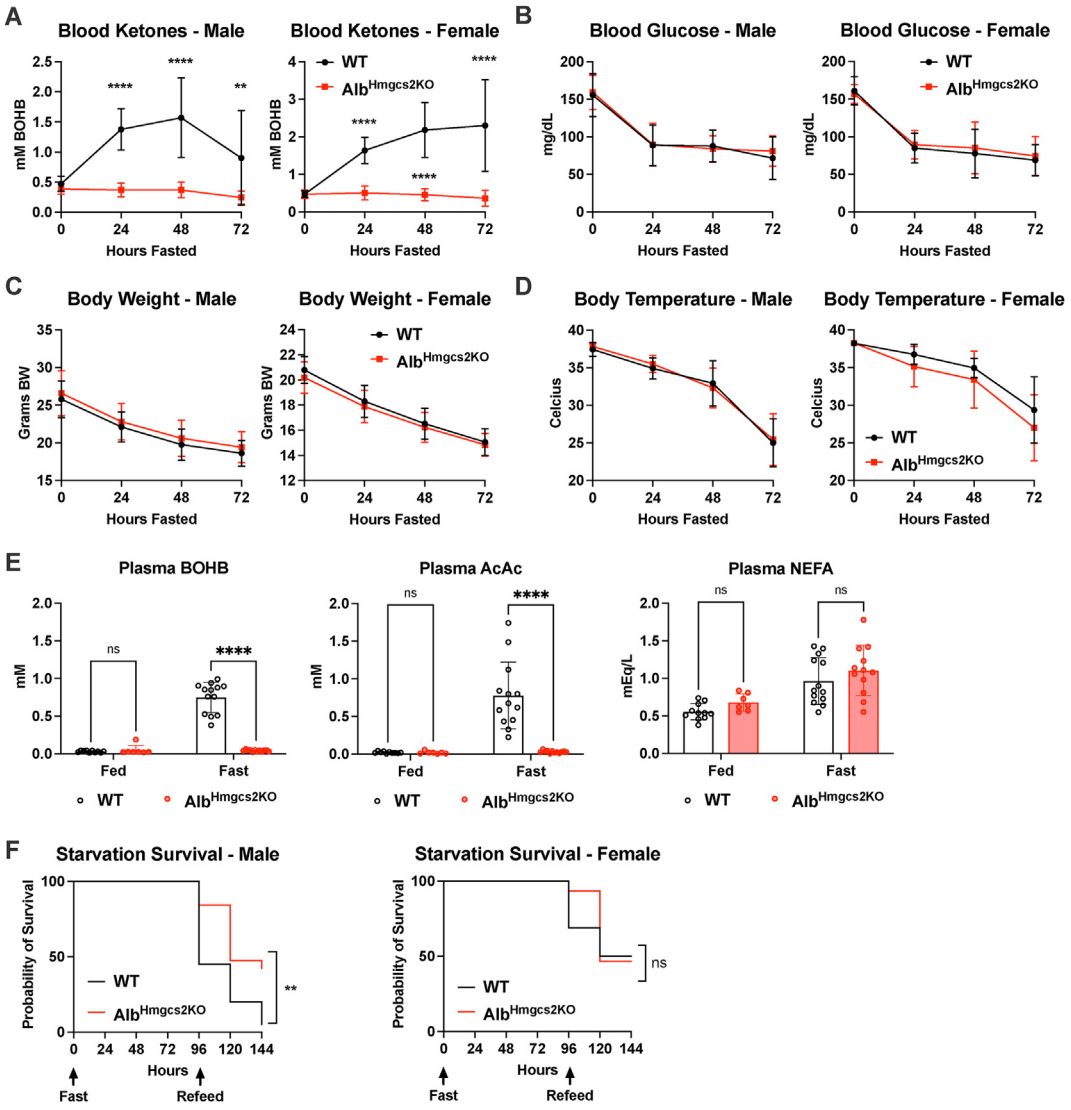

Figure 2: Mice with hepatic ketogenic deficiency do not exhibit any defects in starvation adaptation. **(A–D)** WT and Alb^{Hmgcs2KO} mice were fasted for 72 h n = 19–20/group (male), n = 15–16/group (female). **(A)** Blood ketones, beta-hydroxybutyrate (BOHB) measured by ketone meter. **(B)** Blood glucose. **(C)** Body weight. **(D)** Rectal body temperatures. **(E)** WT and Alb^{Hmgcs2KO} mice were fasted for 24 h. Plasma BOHB and Acetoacetate (AcAc, which was calculated by the difference between total ketones and BOHB) measured by colorimetric assay (Wako), and plasma non esterified fatty acids (NEFA). n = 7–13/group. **(F)** Survival after WT and Alb^{Hmgcs2KO} mice were fasted for 96 h and then refed. n = 19–20/group (male), n = 15–16/group (female). Data expressed as mean ± SD, $^{**}P < 0.01$, $^{****}P < 0.0001$, ns (not significant); two-way ANOVA with Sidak's multiple comparisons test (E) with mixed effects (A–D), Mantel–Cox test (F).

difference in the rate of fat mass loss, fasting lipolysis gene expression [21] in epididymal white adipose tissue was not significantly different in fed and 24-h fasted Alb^{Hmgcs2KO} mice compared to WT mice (Figure 3H). As these experiments were performed two weeks after tamoxifen administration for *Hmgcs2* deletion, we considered the possibility of potential effects of ketogenic deficiency increasing fat mass in male mice prior to fasting and therefore improving starvation survival. Although *Hmgcs2*-targeted ASO treatment for 11 days in postnatal mice and 4 weeks in adult mice resulted in a 70% and 88% decrease in HMGCS2 protein abundance, respectively [18], we found that tamoxifen administration 72 h prior to initiation of fasting decreased hepatic HMGCS2 protein abundance by 87.04 ± 6.64% and was sufficient to induce a 91.74 ± 3.54% decrease in fasting ketones (Figure 4A–C). Ad libitum fed liver TG levels are also no different between Alb^{Hmgcs2KO} mice and wild-type littermates 72 h after tamoxifen administration (Figure 4D). Using this tamoxifen administration schedule, 72 h prior to food removal, we found that male Alb^{Hmgcs2KO} mice no longer had a difference in baseline fat mass. They continued to exhibit not only a similar physiologic fasting adaptation (Figure 4E–L, Supplemental Figure 1B, Supplemental Table 5), but also had improved survival to starvation compared to wild-type littermates (Figure 4M). These data suggest that hepatic ketogenesis is not required to maintain lean muscle mass in starvation adaptation. In male mice, it appears that the lack of fasting ketosis may decrease overall fat mass losses during prolonged fasting and improve survival. It is unclear why induced hepatic *Hmgcs2* deletion 72 h prior to starvation initiation provides an additional survival advantage in male mice. It is possible that the minimal residual HMGCS2 protein and plasma ketones in this rapid deletion model provide more protection than either wild-type preserved HMGCS2 hepatic expression or complete hepatic HMGCS2 loss. More work is needed to determine the mechanism of enhanced survival.

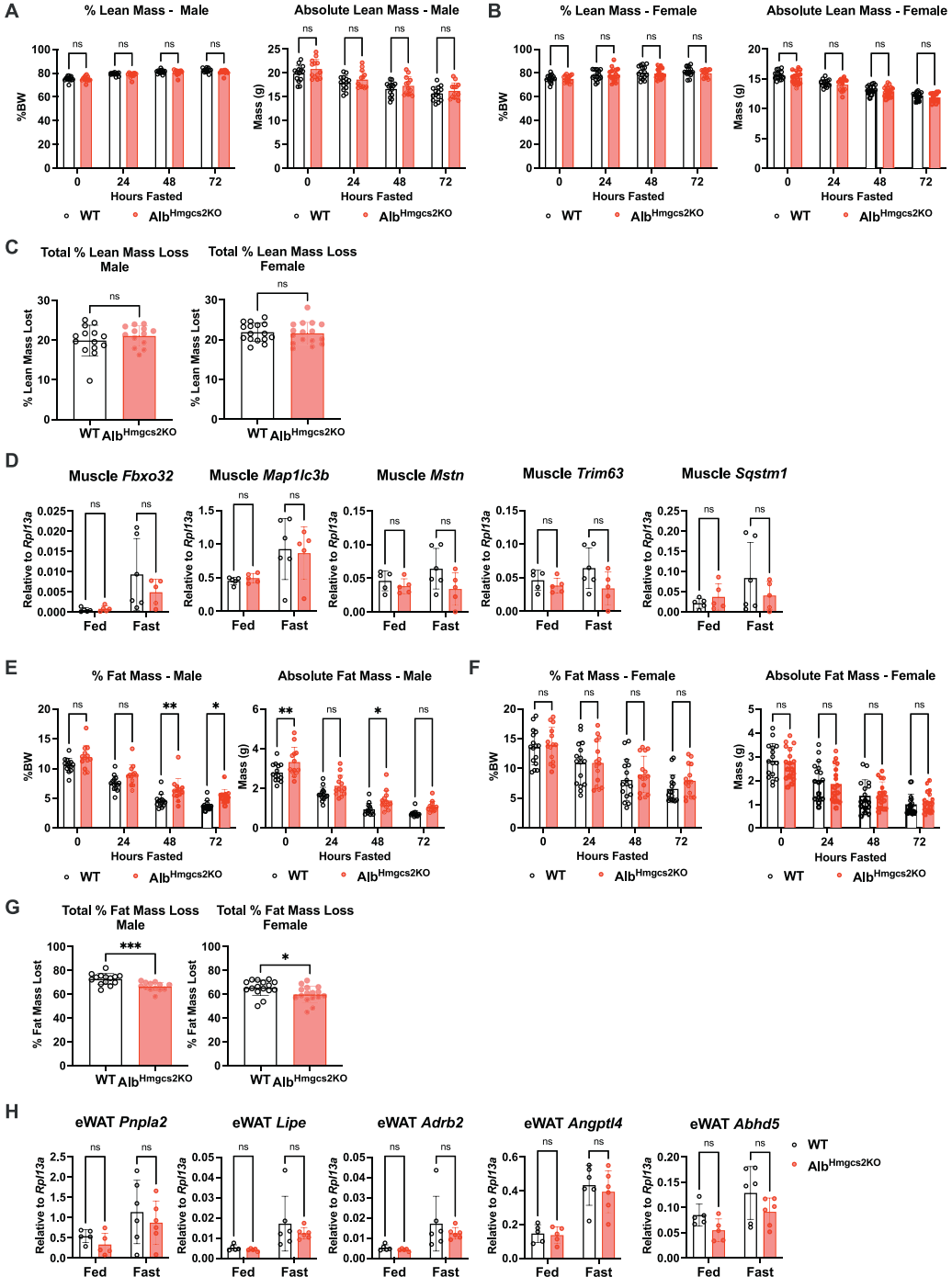

Figure 3: Hepatic ketogenesis does not preserve lean mass during prolonged fasting. WT and Alb^{Hmgcs2KO} mice were fasted for 72 h, two weeks after tamoxifen administration. Fat and lean mass were measured by nuclear magnetic resonance (NMR) at baseline and every 24 h n = 13–14/group (male) n = 15–16/group (female). **(A–B)** Lean mass by percent body weight (BW) and absolute mass. **(C)** Total percent lean mass loss at 72 h of fasting compared to baseline. **(D)** Gastrocnemius skeletal muscle mRNA expression shown relative to *Rpl13a*. **(E–F)** Fat mass by percent body weight and absolute mass. **(G)** Total percent fat mass loss at 72 h of fasting compared to baseline. **(H)** Epididymal white adipose tissue (eWAT) mRNA expression shown relative to *Rpl13a*. Data expressed as mean ± SD, $^{*}P < 0.05$, $^{**}P < 0.01$, $^{***}P < 0.001$, ns (not significant); two-way ANOVA with Sidak's multiple comparisons test (A, B, D–F, H), two-sided, unpaired t test (C, G).

In response to fasting, Alb^{Hmgcs2KO} mice exhibited the expected rise in plasma branched chain amino acids (BCAA) and depletion of alanine and lactate (Figure 5A, D, Supplemental Fig. 2). The fasting-induced decrease in plasma lactate was greater in mice when hepatic *Hmgcs2* deletion was induced 72 h prior to fasting (Figure 5D). Alb^{Hmgcs2KO} mice also demonstrated a trend towards higher levels of plasma BCAA and urea (Figure 5A, B, D, E). Gluconeogenic gene expression also generally trended higher in Alb^{Hmgcs2KO} livers at 24 h of fasting (Figure 5C, F).

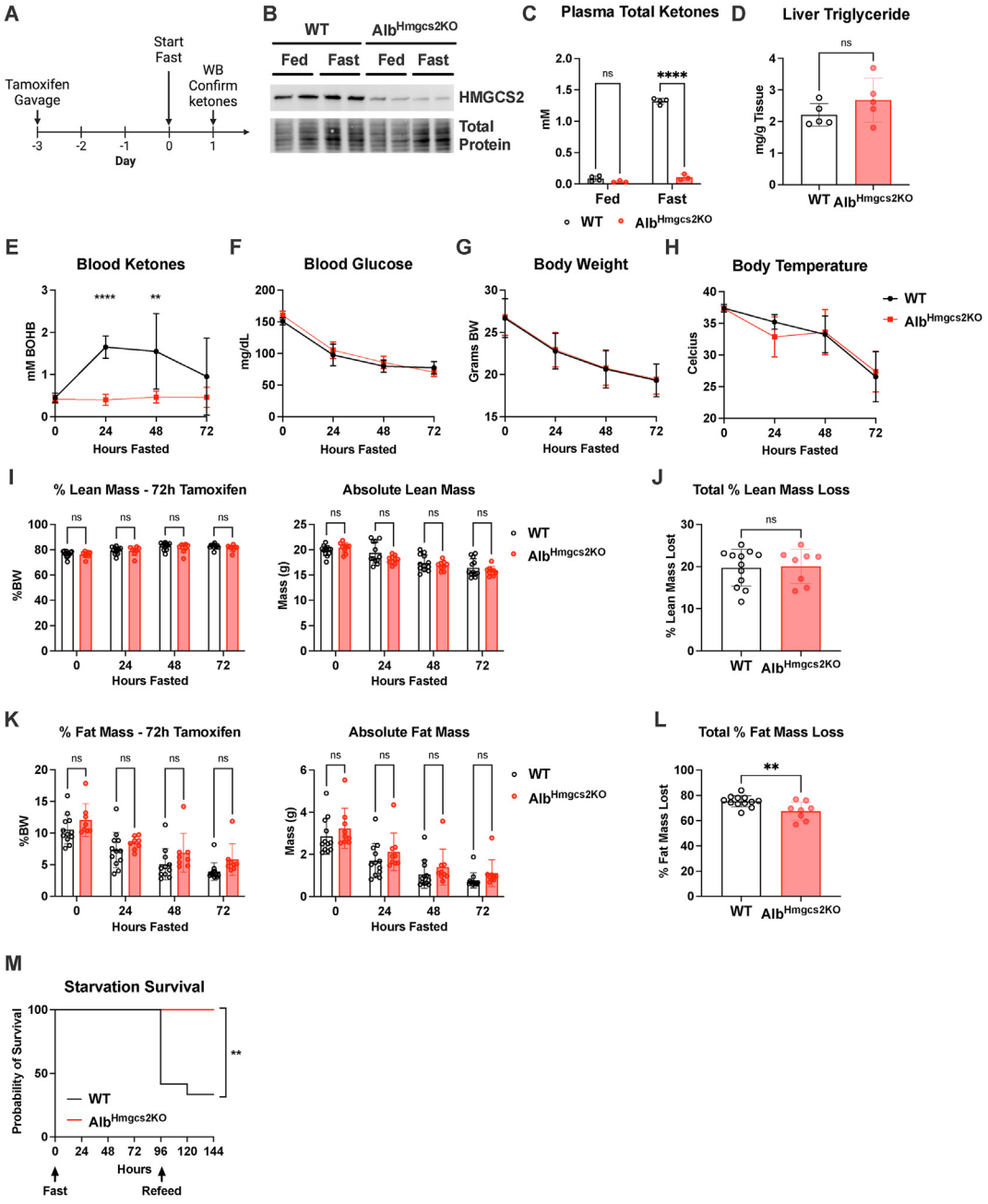

Figure 4: After matching for baseline fat mass, male mice with hepatic ketogenic deficiency have improved survival from prolonged starvation. **(A–C)** WT and Alb^{Hmgcs2KO} male mice were ad libitum fed or fasted for 24 h, 72 h after tamoxifen administration. **(A)** Overview of tamoxifen timing and start of fast for (B, C). **(B)** Whole liver protein lysates immunoblotted for HMGCS2. **(C)** Plasma total ketones measured by colorimetric assay (Wako). n = 3–4/group. **(D)** Liver triglyceride concentrations (mg/g tissue) in ad libitum fed WT and Alb^{Hmgcs2KO} male mice 72 h after tamoxifen administration. n = 5/group. **(E–L)** WT and Alb^{Hmgcs2KO} male mice were fasted 72 h after tamoxifen administration. n = 8–12/group. **(E)** Blood ketones (BOHB ketone meter). **(F)** Blood glucose. **(G)** Body weight. **(H)** Rectal body temperature. **(I–L)** Fat and lean mass were measured by nuclear magnetic resonance (NMR) at baseline and every 24 h. **(I)** Lean mass by percent body weight and absolute mass. **(J)** Total percent lean mass loss at 72 h of fasting compared to baseline. **(K)** Fat mass by percent body weight and absolute mass. **(L)** Total percent fat mass loss at 72 h of fasting compared to baseline. **(M)** Survival after WT and Alb^{Hmgcs2KO} mice were fasted for 96 h and then refed. n = 8–12/group. Data expressed as mean ± SD, $^{**}P < 0.01$, $^{****}P < 0.0001$, ns (not significant); two-way ANOVA with Sidak's multiple comparisons test (C, I, K) with mixed effects (E–H), two-sided, unpaired t test (D, J, L), Mantel–Cox test (M).

These observations suggest that proteolysis may increase to fuel gluconeogenesis in fasting Alb^{Hmgcs2KO} mice. However, since lean mass loss during fasting was not altered by *Hmgcs2* loss, it is unclear whether proteolysis could be sufficient to supplement their systemic intermediary metabolism. As prolonged *Hmgcs2* knockdown leads to an increase in liver glycogen [22], we next considered whether pre-fasting liver glycogen stores in the Alb^{Hmgcs2KO} mice could contribute to the maintenance of fasting glycemia in Alb^{Hmgcs2KO} mice. However, unlike prolonged *Hmgcs2* knockdown, short-term induced deletion of hepatic *Hmgcs2* did not result in higher liver glycogen stores (Figure 5G). In fact,

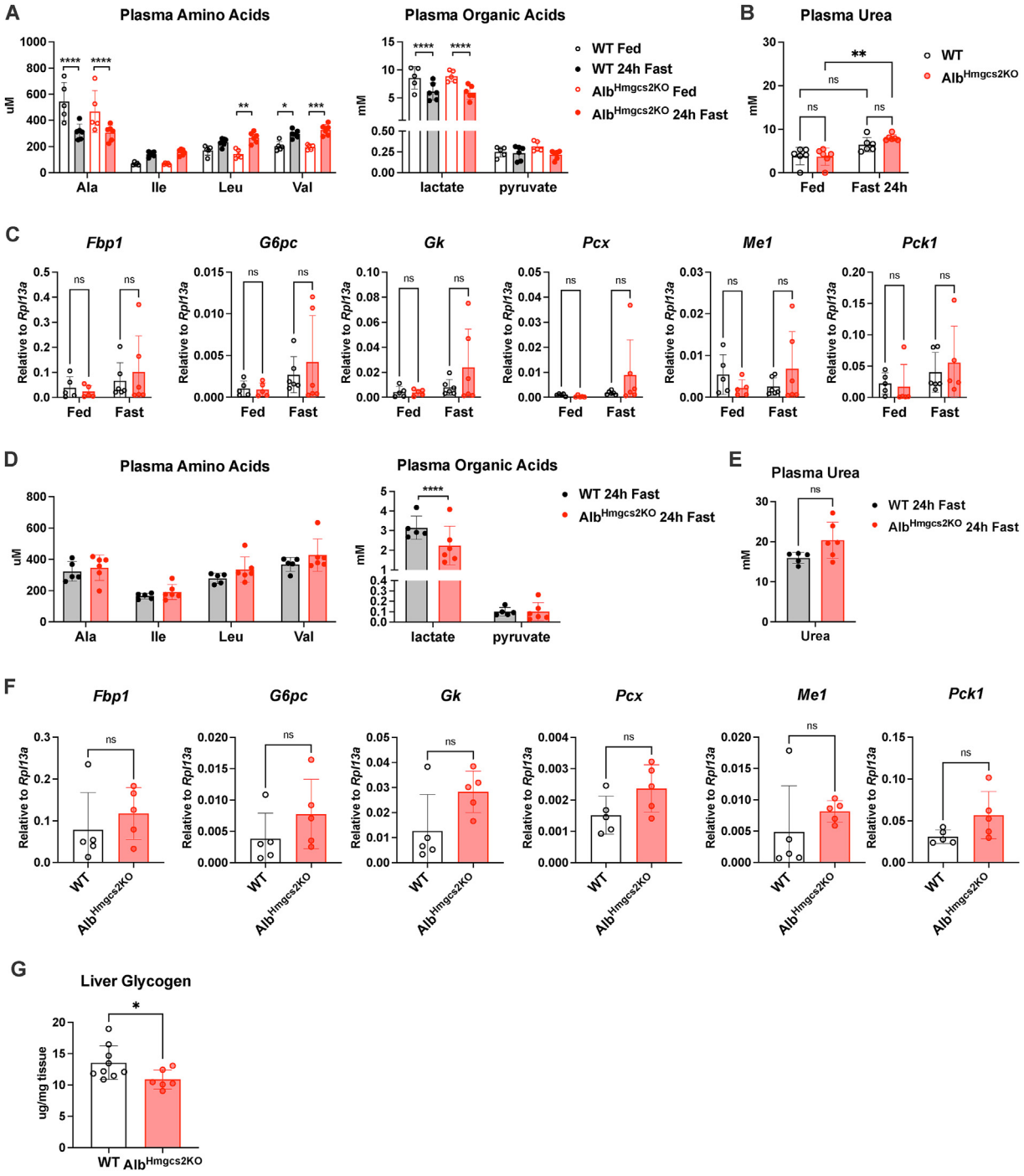

Figure 5: Hepatic ketogenic deficit mice exhibit expected changes in plasma amino acids and organic acids during fasting. **(A–C)** WT and Alb^{Hmgcs2KO} male mice were ad libitum fed or fasted for 24 h 2 weeks after tamoxifen administration. n = 5–6/group. **(A)** Plasma amino and organic acids. **(B)** Plasma urea. **(C)** Liver mRNA expression shown relative to *Rpl13a*. **(D–F)** WT and Alb^{Hmgcs2KO} male mice were fasted for 24 h 72 h after tamoxifen administration. n = 5–6/group. **(D)** Plasma amino and organic acids. **(E)** Plasma urea. **(F)** Liver mRNA expression shown relative to *Rpl13a*. **(G)** Glycogen content measured from livers harvested from ad libitum fed WT and Alb^{Hmgcs2KO} male mice 72 h after tamoxifen administration. n = 6–9/group. Data expressed as mean ± SD, $^{*}P < 0.05$, $^{**}P < 0.01$, $^{***}P < 0.001$, $^{****}P < 0.0001$, ns (not significant); two-way ANOVA with Sidak's multiple comparisons test (A–C), two-sided, unpaired t test (D–G).

the amount of baseline liver glycogen was interestingly lower in Alb^{Hmgcs2KO} mice in the fed state. Thus, Alb^{Hmgcs2KO} mice do not start with more hepatic glycogen stores prior to prolonged starvation. However, whether hepatic ketogenic deficiency alters the rate of hepatic glycogen depletion during fasting remains to be determined.

3.4. Energy expenditure does not explain starvation adaptation in hepatic ketogenic deficiency

As Alb^{Hmgcs2KO} mice preserved both their lean muscle and fat mass while maintaining their blood glucose and body temperature, we next assessed whether they decreased their energy expenditure and activity

to compensate for the lack of ketones. Male and female Alb^{Hmgcs2KO} mice were placed in metabolic chambers to measure energy expenditure and activity before and during a prolonged fast. Compared to wild-type littermates, male Alb^{Hmgcs2KO} mice exhibited a non-significant trend toward increased activity during fasting, but there were no obvious differences in energy expenditure, respiratory exchange ratio (RER), or O_2 and CO_2 balance (Figure 6A, B and Supplemental Figures 3A—C, Fig. 4). Female Alb^{Hmgcs2KO} mice also exhibited no significant differences in energy expenditure or activity compared to WT mice (Figure 6C, D) across the entire fed and fasted periods. When examined during the individual light and dark phases of each 24-h period of fasting, female Alb^{Hmgcs2KO} mice demonstrated a decrease in energy expenditure as well as O_2 consumption and CO_2 production during the final 72 h fasting period compared to wild-type controls (Supplemental Figure 4B, D, E). Female Alb^{Hmgcs2KO} mice also had a significantly, but modestly, higher RER during the entire fasting period, though when examined during each 24-h period, there was no significant difference (Supplemental Figures 3D and 4A). The relatively normal decline in fasting RER in fasting male and female Alb^{Hmgcs2KO} mice is notable since ketogenesis followed by ketone oxidation is indistinguishable from fat oxidation based on O_2/CO_2 balance [23]. This observation indicates that loss of hepatic ketogenesis does not result in a greater reliance on carbohydrate oxidation, which would cause the RER to remain high during fasting, or a more rapid switch to amino acid oxidation, which would cause the RER to drift up more quickly during fasting. Thus, loss of hepatic ketogenesis appears to result in increased fat oxidation without its conversion to ketones by the liver. While female Alb^{Hmgcs2KO} mice decreased their energy expenditure during the latter periods of prolonged fasting, it remains unclear how male Alb^{Hmgcs2KO} mice were able to sustain similar levels of activity while losing less fat mass, maintaining muscle mass and blood glucose, as well as surviving starvation better than control animals.

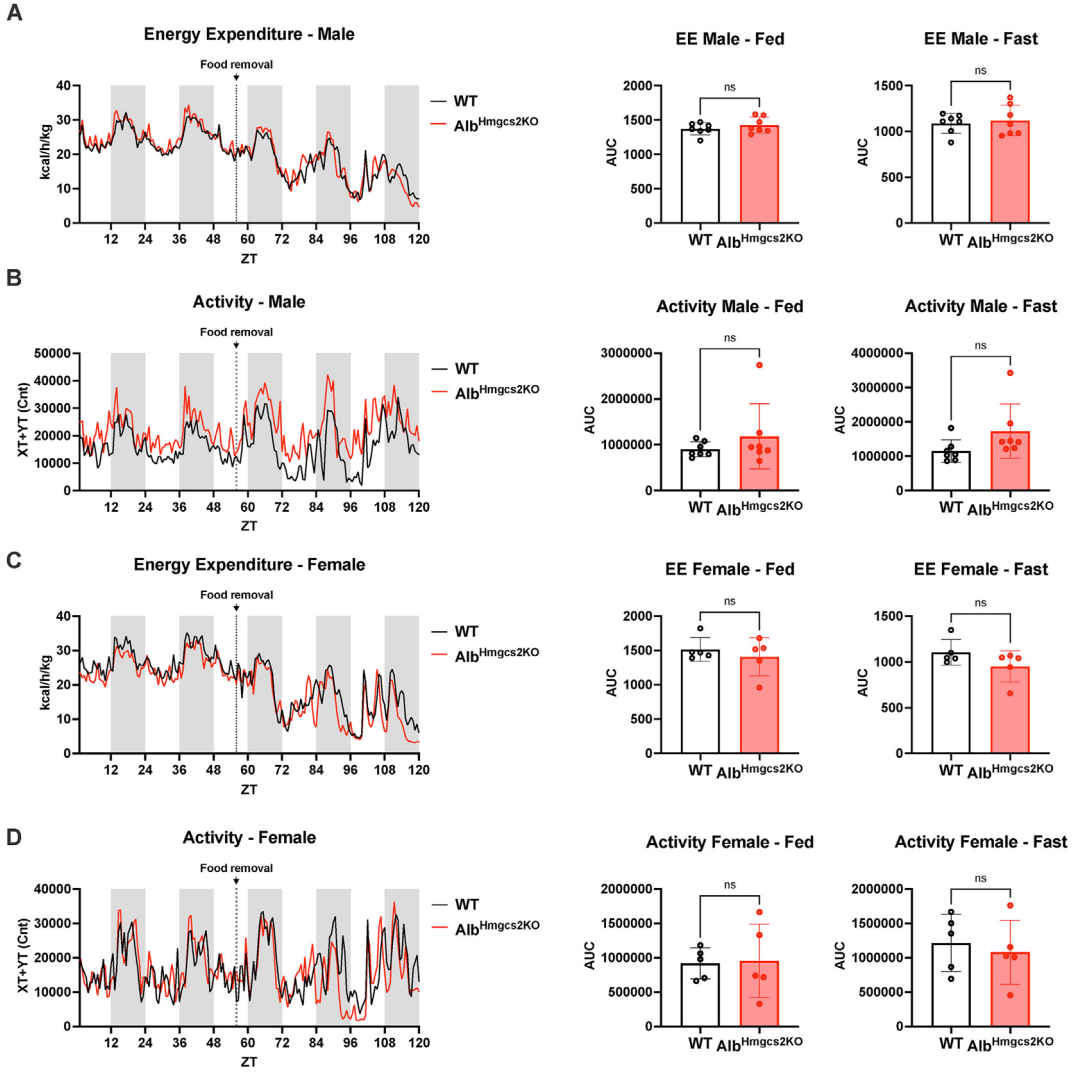

Figure 6: Hepatic ketogenic deficiency does not affect activity or energy expenditure during prolonged fasting. WT and Alb^{Hmgcs2KO} mice were fasted 72 h after tamoxifen administration. (A—B) male mice n = 7/group, (C—D) female mice n = 5/group. **(A, C)** Energy expenditure (EE) and area under the curve (AUC) calculated during the fed and fasted periods. **(B, D)** Activity and area under the curve (AUC) calculated during the fed and fasted periods. Data expressed as mean ± SD, ns (not significant); two-sided, unpaired t test (A—D).

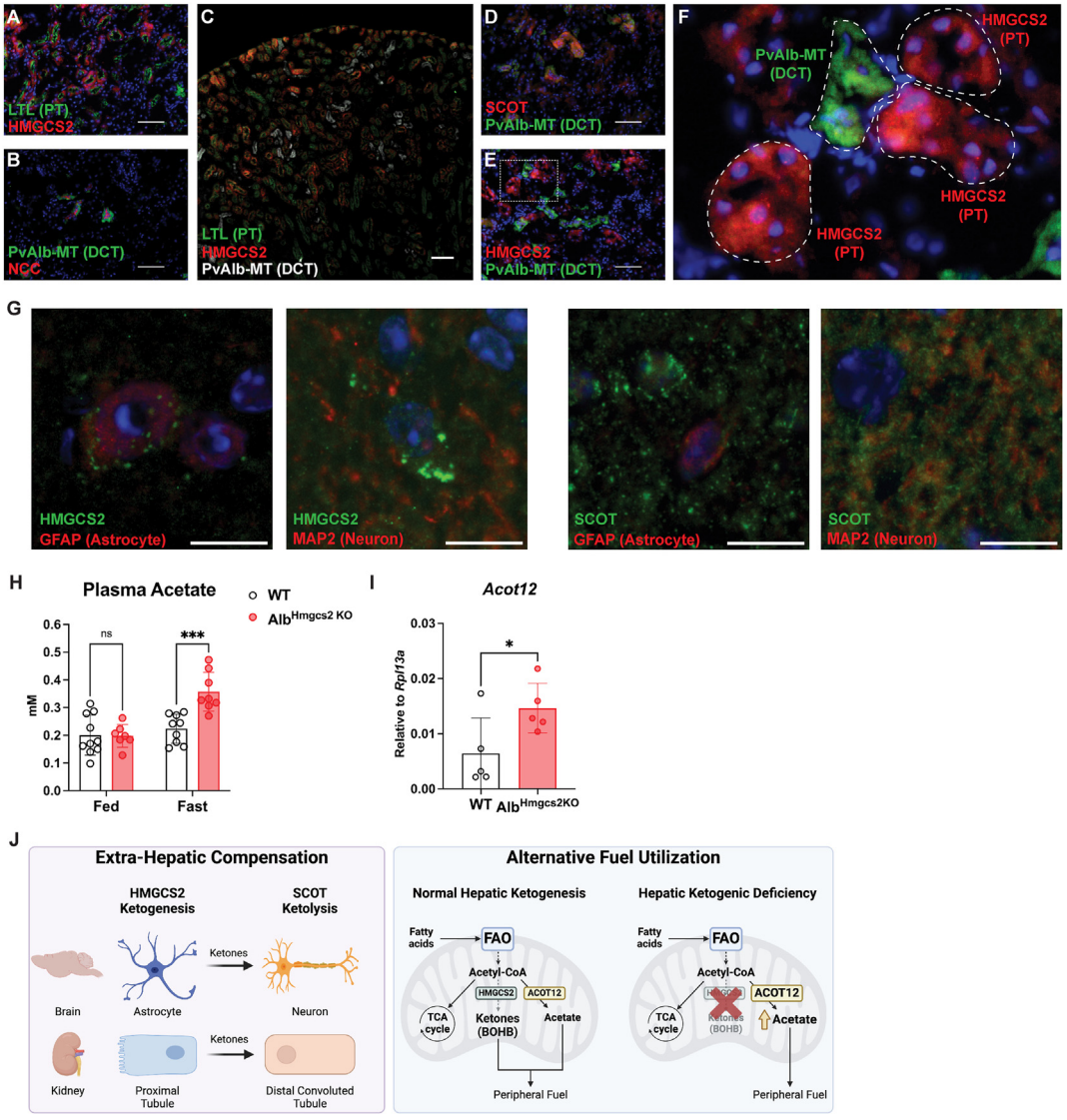

Figure 7: Alternative pathways of metabolic compensation. **(A–F)** Immunostaining of kidney sections from 24-h fasted wild-type mice using various co-staining comparisons: Lotus lectin (LTL), a proximal tubule (PT) marker; anti-HMGCS2; anti-GFP against a reporter mouse (PvAlb-MT) for the distal convoluted tubule (DCT); anti-sodium chloride co-transporter (NCC, a DCT marker), and/or anti-SCOT. **(F)** represents region indicated in **(E)**. Scale bar represents 100 μm. **(G)** Immunostaining of brain sections (midbrain, anterior to the hypothalamus) from ad libitum fed wild-type mice using various co-staining comparisons: anti-glial fibrillary acidic protein (GFAP, an astrocyte marker), anti-microtubule-associated protein 2 (MAP-2, a neuronal marker), and anti-HMGCS2. Scale bar represents 30 μm. **(H)** WT and $Alb^{Hmgcs2KO}$ mice were fasted for 24 h or fed ad libitum, 72 h after tamoxifen administration. Plasma acetate levels measured by GC/MS. n = 7–10/group. **(I)** WT and $Alb^{Hmgcs2KO}$ mice were fasted for 24 h, 72 h after tamoxifen administration. Liver mRNA shown relative to *Rpl13a*. n = 5/group. Data expressed as mean ± SD, $*P < 0.05$, $***P < 0.001$, ns (not significant); two-way ANOVA with Sidak's multiple comparisons test (H), two-sided, unpaired t test (I). **(J)** Model of fasting metabolic compensation in hepatic ketogenic deficiency. Image created by BioRender.com.

3.5. Potential fasting metabolic compensation in hepatic ketogenic deficiency

As fasting ketosis is considered essential for mammalian starvation adaptation, the observation that mice lacking hepatic *Hmgcs2* lose the ability to generate fasting ketosis but successfully adapt to starvation is unexpected. Loss of function *HMGCS2* mutations in humans results in hypoketotic hypoglycemia that rapidly leads to hypoglycemic coma within 18–22 h of fasting [24,25]. Global *Hmgcs2* knockout (KO) mice have been described to demonstrate significant postnatal mortality [17]. The ability of $Alb^{Hmgcs2KO}$ mice to adapt to starvation without significant hypoglycemia or loss of lean mass suggests an alternative mechanism of metabolic compensation for the lack of hepatic ketogenesis. In contrast to human patients with germline mutations in *HMGCS2* and mice with global *Hmgcs2* deletion affecting all cell types, extra-hepatic *Hmgcs2* expression could compensate for the lack of liver-derived circulating ketones in our hepatic-specific *Hmgcs2* knockout mouse model.

As $Alb^{Hmgcs2KO}$ mice do not develop fasting ketosis, other organs that express HMGCS2, including the brain, heart, intestine, and kidney [5,26–28], do not contribute to the circulating ketone pool, neither in normal conditions nor in the context of hepatic ketogenic deficiency [5]. However, HMGCS2 expression is preserved in these extrahepatic organs in the $Alb^{Hmgcs2KO}$ mice (Figure 1D), suggesting the possibility that local ketones could be generated for local use. In the context of

hepatic ketogenic deficiency, certain extrahepatic tissues that utilize ketones for energy could compensate for the lack of liver-derived ketones by expressing HMGCS2 in select cellular populations and generating their own ketones for consumption in other cell types that utilize ketones for energy. From a systemic view, this process would be indistinguishable from fat oxidation, but it has mechanistic implications for cellular compartments that may not be equipped for long chain fatty acid metabolism. In the kidney, fasting-induced HMGCS2 expression in the proximal tubule is spatially adjacent to distal convoluted tubular cells that highly express Succinyl-CoA:3-oxoacid CoA transferase (SCOT), the rate limiting enzyme for ketolysis (Figure 7A–F, Supplemental Figure 5). This anatomic proximity of different cell types with differential HMGCS2 and SCOT expression suggests the possibility of proximal tubular ketone production for the utilization by the distal convoluted tubule. In the brain, astrocytes highly express HMGCS2 [29]. Indeed, we also found HMGCS2 expressing astrocytes in the brain while neighboring neurons express SCOT (Figure 7G). It has been postulated that astrocytes produce ketones to fuel neurons based on primary culture studies [26,27,30], non-specific pharmacologic inhibition of both HMGCS2 and the cytosolic isoform HMGCS1 involved in cholesterol synthesis [31], and genetic knockdown of *Drosophila Hmgs*, the ortholog to mammalian *HMGCS1* [32]. However, these studies did not definitively show mitochondrial expression of the HMGCS2 isoform, mitochondrial HMGCS activity, and in vivo de novo ketogenesis in astrocytes.

Thus, a more likely explanation for normal starvation adaptation in hepatic ketogenic deficiency is the activation of other fasting metabolic adaptation pathways and use of alternative fuels. Data from mouse models targeting *Oxct1*, the gene encoding the ketolytic enzyme SCOT, suggest such a relationship. Germline deletion of *Oxct1* with a systemic inability to utilize ketones for energy is neonatal lethal while mice with single tissue specific *Oxct1* deletion in the cardiomyocytes, skeletal myocytes, or neurons are all viable as neonates and can maintain their blood glucose during a 48-h fast as adults [33,34], suggesting these organs could utilize a non-ketone fuel. Interestingly, there are rare mammalian examples in which ketogenesis is not required for starvation adaptation. Investigation of the evolution of the *HMGCS2* gene identified three mammalian lineages that have lost the *HMGCS2* gene, including cetaceans [35]. Bottlenose dolphins can survive prolonged fasting and maintain high blood glucose levels despite the inability to produce ketone bodies [36,37]. While it is unknown how cetaceans adapt to starvation without ketogenesis, the use of an alternate fuel is likely. As the liver will co-produce acetate with ketone bodies, acetate could be a candidate alternate fuel [38–40]. In fact, hepatic mRNA expression of Acyl-CoA Thioesterase 12 (*Acot12*), which catalyzes the conversion of acetyl-CoA to acetate, and plasma acetate levels were significantly higher in $Alb^{Hmgcs2KO}$ mice in response to fasting (Figure 7H, I), suggesting that in the absence of hepatic ketogenesis, acetate could serve as an alternate fuel for starvation adaptation. The fasting-induced rise in blood acetate concentration (0.2 mM) is small, compared to ketones (1 mM), but its concentration may not reflect its total turnover.

Alternative use of fuels could also explain the observed developmental dimorphism of fasting-induced ketogenesis in some mammals. Northern elephant seals demonstrate developmental differences in ketogenesis during fasting, in which ketogenesis is observed in fasting neonatal pups, while adults fasted for up to 12 weeks exhibit minimal circulating ketone levels [41,42]. Moreover, clinical case series report that patients with HMGCS2 deficiency presented in the first or second year of life with hypoglycemic hypoketotic coma but then after the age of 5, had no further metabolic decompensation and were able to tolerate normal lengths of fasting [43]. In the mouse model of global *Hmgcs2* KO [17] compared to induced hepatic *Hmgcs2* deletion in adult mice in this study, the differences in the effect of ketogenic deficiency on starvation adaptation and survival could also reflect a component of developmental dimorphism. Interestingly, the development of hepatic steatosis with short-term knockdown also differs in neonates versus adult mice [18]. While these phenotypic differences could reflect the difference in dietary intake (high fat breast milk as neonates versus adult low fat chow), one could speculate that ketogenesis is more essential in early development rather than in adulthood when alternative metabolic pathways can mediate starvation adaptation.

Ketones also exhibit signaling properties independent of their function as an alternate fuel. BOHB can participate in post-translational modifications both as an HDAC inhibitor, increasing histone acetylation [44], and as a direct histone modifier, leading to lysine β-hydroxybutyrylation [45]. Ketones can also signal via G-protein coupled receptors GPR41 [46] and GPR109A [47]. The observation that hepatic ketogenic deficient mice can adapt and survive endotoxemia and prolonged starvation suggests that both fuel and non-fuel signaling functions of ketones are dispensable in these contexts. In male mice, hepatic ketogenesis may be a liability in starvation adaptation, the mechanism of which remains to be determined.

4. CONCLUSION

While anorexia-induced fasting metabolism appears to be protective in bacterial inflammation, circulating hepatic-derived ketones do not participate in mediating the survival benefit. Our findings suggest that circulating ketones may act merely as biomarkers of the fasting-induced metabolic programs that mediate the protective effects of sickness-induced anorexia. As hepatic deficient mice also do not exhibit a defect in starvation adaptation, the surprising capacity for metabolic compensation raises additional possibilities of extrahepatic ketogenesis and the use of alternative fuels (Figure 7J). Future work is needed to establish the mechanisms of metabolic compensation allowing for the maintenance of fasting glycemia and lean muscle mass in hepatic ketogenesis deficiency and to determine how sex and developmental stage modify physiologic plasticity and metabolic flexibility in starvation adaptation.

CREDIT AUTHORSHIP CONTRIBUTION STATEMENT

Kyle Feola: Writing — review & editing, Writing — original draft, Visualization, Methodology, Investigation, Formal analysis, Conceptualization. **Andrea H. Venable:** Investigation, Formal analysis. **Tatyana Broomfield:** Investigation. **Morgan Villegas:** Investigation. **Xiaorong Fu:** Methodology, Investigation. **Shawn Burgess:** Writing — review & editing, Methodology, Formal analysis. **Sarah C. Huen:** Writing — review & editing, Writing — original draft, Visualization, Methodology, Funding acquisition, Formal analysis, Conceptualization.

ACKNOWLEDGMENTS

We thank Drs. David Mangelsdorf and Steven Kliewer for helpful discussions and review of the manuscript. We thank Jessica Sudderth for the measurements of plasma acetate. Support was provided by National Institute of General Medical Sciences Grant R35GM137984 (S.C.H.); National Institute of Diabetes and Digestive and Kidney Diseases T32 Training Grant T32DK007257 (A.H.V); Dr. Robert C. and

Veronica Atkins Foundation (S.B.); and the UT Southwestern NORC Metabolic Phenotyping and Quantitative Metabolism Cores (NIH P30DK127984).

DECLARATION OF COMPETING INTEREST

The authors declare that they have no known competing financial interests or personal relationships that could have appeared to influence the work reported in this paper.

DATA AVAILABILITY

Data will be made available on request.

APPENDIX A. SUPPLEMENTARY DATA

Supplementary data to this article can be found online at https://doi.org/10.1016/j.molmet.2024.101967.

REFERENCES

[1] Hart BL. Biological basis of the behavior of sick animals. Neurosci Biobehav Rev 1988;12:123—37.
[2] Wang A, Huen SC, Luan HH, Yu S, Zhang C, Gallezot JD, et al. Opposing effects of fasting metabolism on tissue tolerance in bacterial and viral inflammation. Cell 2016;166:1512—1525.e12.
[3] Wang A, Huen SC, Luan HH, Baker K, Rinder H, Booth CJ, et al. Glucose metabolism mediates disease tolerance in cerebral malaria. Proc Natl Acad Sci U S A 2018;115:11042—7.
[4] Puchalska P, Crawford PA. Multi-dimensional roles of ketone bodies in fuel metabolism, signaling, and therapeutics. Cell Metab 2017;25:262—84.
[5] Venable AH, Lee LE, Feola K, Santoyo J, Broomfield T, Huen SC. Fasting-induced HMGCS2 expression in the kidney does not contribute to circulating ketones. Am J Physiol Ren Physiol 2022;322:F460—7.
[6] Bayraktar EC, Baudrier L, Özerdem C, Lewis CA, Chan SH, Kunchok T, et al. MITO-tag mice enable rapid isolation and multimodal profiling of mitochondria from specific cell types in vivo. Proc Natl Acad Sci U S A 2019;116:303—12.
[7] Hippenmeyer S, Vrieseling E, Sigrist M, Portmann T, Laengle C, Ladle DR, et al. A developmental switch in the response of DRG neurons to ETS transcription factor signaling. PLoS Biol 2005;3:e159.
[8] Belge H, Gailly P, Schwaller B, Loffing J, Debaix H, Riveira-Munoz E, et al. Renal expression of parvalbumin is critical for NaCl handling and response to diuretics. Proc Natl Acad Sci U S A 2007;104:14849—54.
[9] Casetta B, Tagliacozzi D, Shushan B, Federici G. Development of a method for rapid quantitation of amino acids by liquid chromatography-tandem mass spectrometry (LC-MSMS) in plasma. Clin Chem Lab Med 2000;38:391—401.
[10] Des Rosiers C, Fernandez CA, David F, Brunengraber H. Reversibility of the mitochondrial isocitrate dehydrogenase reaction in the perfused rat liver. Evidence from isotopomer analysis of citric acid cycle intermediates. J Biol Chem 1994;269:27179—82.
[11] Tumanov S, Bulusu V, Gottlieb E, Kamphorst JJ. A rapid method for quantifying free and bound acetate based on alkylation and GC-MS analysis. Cancer Metab 2016;4:17.
[12] Folch J, Lees M, Stanley GHS. A simple method for the isolation and purification of total lipides from animal tissues. J Biol Chem 1956;226:497—509.
[13] Takeyama N, Itoh Y, Kitazawa Y, Tanaka T. Altered hepatic mitochondrial fatty acid oxidation and ketogenesis in endotoxic rats. Am J Physiol 1990;259:E498—505.
[14] Vary TC, Siegel JH, Nakatani T, Sato T, Aoyama H. A biochemical basis for depressed ketogenesis in sepsis. J Trauma 1986;26:419—25.
[15] Lanza-Jacoby S, Rosato E, Braccia G, Tabares A. Altered ketone body metabolism during gram-negative sepsis in the rat. Metabolism 1990;39:1151—7.
[16] Ago Y, Otsuka H, Sasai H, Abdelkreem E, Nakama M, Aoyama Y, et al. Japanese patients with mitochondrial 3-hydroxy-3-methylglutaryl-CoA synthase deficiency: in vitro functional analysis of five novel HMGCS2 mutations. Exp Ther Med 2020;20:39.
[17] Asif S, Kim RY, Fatica T, Sim J, Zhao X, Oh Y, et al. Hmgcs2-mediated ketogenesis modulates high-fat diet-induced hepatosteatosis. Mol Metab 2022;61:101494.
[18] Cotter DG, Ercal B, Huang X, Leid JM, d'Avignon DA, Graham MJ, et al. Ketogenesis prevents diet-induced fatty liver injury and hyperglycemia. J Clin Investig 2014;124:5175—90.
[19] Cahill GF. President's address. Starvation. Trans Am Clin Climatol Assoc 1983;94:1—21.
[20] Hildebrandt AL, Neufer PD. Exercise attenuates the fasting-induced transcriptional activation of metabolic genes in skeletal muscle. Am J Physiol Endocrinol Metab 2000;278:E1078—86.
[21] Defour M, Michielsen CCJR, O'Donovan SD, Afman LA, Kersten S. Transcriptomic signature of fasting in human adipose tissue. Physiol Genom 2020;52:451—67.
[22] d'Avignon DA, Puchalska P, Ercal B, Chang Y, Martin SE, Graham MJ, et al. Hepatic ketogenic insufficiency reprograms hepatic glycogen metabolism and the lipidome. JCI Insight 2018;3:99762.
[23] Fernández-Verdejo R, Mey JT, Ravussin E. Effects of ketone bodies on energy expenditure, substrate utilization, and energy intake in humans. J Lipid Res 2023;64:100442.
[24] Thompson GN, Hsu BY, Pitt JJ, Treacy E, Stanley CA. Fasting hypoketotic coma in a child with deficiency of mitochondrial 3-hydroxy-3-methylglutaryl-CoA synthase. N Engl J Med 1997;337:1203—7.
[25] Morris AA, Lascelles CV, Olpin SE, Lake BD, Leonard JV, Quant PA. Hepatic mitochondrial 3-hydroxy-3-methylglutaryl-coenzyme a synthase deficiency. Pediatr Res 1998;44:392—6.
[26] Blázquez C, Woods A, de Ceballos ML, Carling D, Guzmán M. The AMP-activated protein kinase is involved in the regulation of ketone body production by astrocytes. J Neurochem 1999;73:1674—82.
[27] Thevenet J, De Marchi U, Domingo JS, Christinat N, Bultot L, Lefebvre G, et al. Medium-chain fatty acids inhibit mitochondrial metabolism in astrocytes promoting astrocyte-neuron lactate and ketone body shuttle systems. FASEB J 2016;30:1913—26.
[28] Wentz AE, d'Avignon DA, Weber ML, Cotter DG, Doherty JM, Kerns R, et al. Adaptation of myocardial substrate metabolism to a ketogenic nutrient environment. J Biol Chem 2010;285:24447—56.
[29] Jurga AM, Paleczna M, Kadluczka J, Kuter KZ. Beyond the GFAP-astrocyte protein markers in the brain. Biomolecules 2021;11:1361.
[30] Auestad N, Korsak RA, Morrow JW, Edmond J. Fatty acid oxidation and ketogenesis by astrocytes in primary culture. J Neurochem 1991;56:1376—86.
[31] Le Foll C, Dunn-Meynell AA, Miziorko HM, Levin BE. Regulation of hypothalamic neuronal sensing and food intake by ketone bodies and fatty acids. Diabetes 2014;63:1259—69.
[32] Silva B, Mantha OL, Schor J, Pascual A, Plaçais PY, Pavlowsky A, et al. Glia fuel neurons with locally synthesized ketone bodies to sustain memory under starvation. Nat Metab 2022;4:213—24.
[33] Cotter DG, d'Avignon DA, Wentz AE, Weber ML, Crawford PA. Obligate role for ketone body oxidation in neonatal metabolic homeostasis. J Biol Chem 2011;286:6902—10.
[34] Cotter DG, Schugar RC, Wentz AE, André d'Avignon D, Crawford PA. Successful adaptation to ketosis by mice with tissue-specific deficiency of ketone body oxidation. Am J Physiol Endocrinol Metab 2013;304:E363—74.

[35] Jebb D, Hiller M. Recurrent loss of HMGCS2 shows that ketogenesis is not essential for the evolution of large mammalian brains. eLife 2018;7:e38906.
[36] Ridgway SH. A mini review of dolphin carbohydrate metabolism and suggestions for future research using exhaled air. Front Endocrinol 2013;4:152.
[37] Houser DS, Derous D, Douglas A, Lusseau D. Metabolic response of dolphins to short-term fasting reveals physiological changes that differ from the traditional fasting model. J Exp Biol 2021;224:jeb238915.
[38] Yamashita H, Kaneyuki T, Tagawa K. Production of acetate in the liver and its utilization in peripheral tissues. Biochim Biophys Acta 2001;1532:79—87.
[39] Moffett JR, Puthillathu N, Vengilote R, Jaworski DM, Namboodiri AM. Acetate revisited: a key biomolecule at the nexus of metabolism, epigenetics and oncogenesis-part 1: acetyl-CoA, acetogenesis and acyl-CoA short-chain synthetases. Front Physiol 2020;11:580167.
[40] Wang J, Wen Y, Zhao W, Zhang Y, Lin F, Ouyang C, et al. Hepatic conversion of acetyl-CoA to acetate plays crucial roles in energy stress. eLife 2023;12:RP87419.
[41] Castellini MA, Costa DP. Relationships between plasma ketones and fasting duration in neonatal elephant seals. Am J Physiol 1990;259:R1086—9.
[42] Houser DS, Crocker DE, Tift MS, Champagne CD. Glucose oxidation and nonoxidative glucose disposal during prolonged fasts of the northern elephant seal pup (*Mirounga angustirostris*). Am J Physiol Regul Integr Comp Physiol 2012;303:R562—70.
[43] Pitt JJ, Peters H, Boneh A, Yaplito-Lee J, Wieser S, Hinderhofer K, et al. Mitochondrial 3-hydroxy-3-methylglutaryl-CoA synthase deficiency: urinary organic acid profiles and expanded spectrum of mutations. J Inherit Metab Dis 2015;38:459—66.
[44] Shimazu T, Hirschey MD, Newman J, He W, Shirakawa K, Le Moan N, et al. Suppression of oxidative stress by β-hydroxybutyrate, an endogenous histone deacetylase inhibitor. Science 2013;339:211—4.
[45] Xie Z, Zhang D, Chung D, Tang Z, Huang H, Dai L, et al. Metabolic regulation of gene expression by histone lysine β-hydroxybutyrylation. Mol Cell 2016;62:194—206.
[46] Kimura I, Inoue D, Maeda T, Hara T, Ichimura A, Miyauchi S, et al. Short-chain fatty acids and ketones directly regulate sympathetic nervous system via G protein-coupled receptor 41 (GPR41). Proc Natl Acad Sci U S A 2011;108:8030—5.
[47] Taggart AK, Kero J, Gan X, Cai TQ, Cheng K, Ippolito M, et al. D)-beta-Hydroxybutyrate inhibits adipocyte lipolysis via the nicotinic acid receptor PUMA-G. J Biol Chem 2005;280:26649—52.

